4246 *Chem. Mater.* **2010,** *22,* 4246–4253
DOI:10.1021/cm1008812

CHEMISTRY OF MATERIALS
Article

Supercritical Chemical Fluid Deposition of InP and InAs

Gabriele Aksomaityte,[†] Fei Cheng,[‡] Andrew L. Hector,*[,‡] Jason R. Hyde,[†] William Levason,[‡] Gillian Reid,[‡] David C. Smith,*[,†] James W. Wilson,[†] and Wenjian Zhang[‡]

[†]*School of Physics and Astronomy and* [‡]*School of Chemistry, University of Southampton, Southampton SO17 1BJ, United Kingdom*

Received March 27, 2010. Revised Manuscript Received May 17, 2010

Supercritical chemical fluid deposition (SCFD) from [^{n}Bu$_2$In(μ-E^{t}Bu$_2$)$_2$In^{n}Bu$_2$] precursors (E = P or As) dissolved in a homogeneous hexane/CO_2 fluid results in the growth of a thin film of InP or InAs with a thick mat of nanowires attached to the surface. InP films were well-adhered to the substrate and the nanowires can be removed without disrupting the film; however, the InAs films were poorly adhered, being dislodged simply by tapping the substrate. In many cases, the InP nanowires are single crystalline, and both the nanowires and the underlying films exhibit band-edge luminescence. Use of supercritical CHF_3 as the delivery solvent also leads to good quality InP films and reduced carbon incorporation into the films. The single-source precursor system was responsible for significant amounts of carbon. This work shows that the SCFD method may be generally applicable to the growth of compound semiconductors, with important implications for growth of these materials in confined environments.

Introduction

Although silicon and germanium are the dominant semiconductors in the electronics industry, III−V semiconductor devices still form a huge global market. In particular III−V semiconductors such as GaAs and InP are dominant in RF devices where their high carrier mobilities are key. Another area in which they dominate, due to their direct bandgap and better stability compared with II−VI semiconductors, is optoelectronics and particularly light emitting diodes including the laser diodes used for optical data storage discs. Due to the technological importance of III−V semiconductors, methods for their deposition, particularly molecular beam epitaxy (MBE) and metal−organic chemical vapor deposition (MOCVD), are highly refined and capable of producing material of extremely high purity with monolayer control over layer thicknesses. It is this latter capability which led to the first nanotechnology revolution with a wide range of nanostructures such as quantum wells, wires and dots being produced.

While semiconductor nanostructures produced using orthodox techniques such as MBE and MOCVD are dominant industrially, considerable research effort is being expended in developing novel methods for producing semiconductor nanostructures in order to reduce costs and open up new nanostructure morphologies. One particularly well developed field is that of colloidal semiconductor quantum dots, produced by arrested precipitation, for applications such as biological tags, phosphors and solar cells.[1,2] Another important field is the production of semiconductor nanowires using metal nanoparticle seeds[3,4] for applications in sensing[5] and solar cells.[6] More morphologically complex self-assembled structures are also being developed, e.g. wire-dot heterostructures[7] and hyperbranched nanoparticles.[8]

The self-assembly techniques for producing semiconductor nanostructures already discussed exploit, and to a limited extent manipulate, the natural growth habit of the materials. One promising route to even more complex structures is the in-filling of preformed templates where the form of the nanostructure and the material can be decoupled. A wide range of templates now exist including artificial opals,[9] liquid crystal templated mesoporous materials,[10] microporous materials[11] and even photonic

*Corresponding author. E-mail: a.l.hector@soton.ac.uk; d.c.smith@soton.ac.uk.

(1) (a) Cozzoli, P. D.; Pellegrino, T.; Manna, L. *Chem. Soc. Rev.* **2006**, *35*, 1195. (b) Murray, C. B.; Norris, D. J.; Bawendi, M. G. *J. Am. Chem. Soc.* **1993**, *115*, 8706.
(2) Parak, W. J.; Gerion, D.; Pellegrino, T.; Zanchet, D.; Micheel, C.; Williams, S. C.; Boudreau, R.; Le Gros, M. A.; Larabell, C. A.; Alivisatos, A. P. *Nanotechnology* **2003**, *14*, R15.
(3) (a) Gudiksen, M. S.; Lauhon, L. J.; Wang, J.; Smith, D. C.; Lieber, C. M. *Nature* **2002**, *415*, 617. (b) Wagner, R. S.; Ellis, W. C. *Appl. Phys. Lett.* **1964**, *4*, 89.
(4) (a) Trentler, T. J.; Hickman, K. M.; Goel, S. C.; Viano, A. M.; Gibbons, P. C.; Buhro, W. E. *Science* **1995**, *270*, 1791. (b) Strupeit, T.; Klinke, C.; Kornowski, A.; Weller, H. *ACS Nano* **2009**, *3*, 668. (c) Dorn, A.; Allen, P. M.; Bawendi, M. G. *ACS Nano* **2009**, *3*, 3260.
(5) Tian, B. Z.; Zheng, X. L.; Kempa, T. J.; Fang, Y.; Yu, N. F.; Yu, G. H.; Huang, J. L.; Lieber, C. M. *Nature* **2007**, *449*, 885.
(6) Cui, Y; Wei, Q. Q.; Park, H. K. *Science* **2001**, *293*, 1289.
(7) Müller, J.; Lupton, J. M.; Lagoudakis, P. G.; Schindler, F.; Koeppe, R.; Rogach, A. L.; Feldmann, J.; Talapin, D. V.; Weller, H. *Nano Lett.* **2005**, *5*, 2044.
(8) Kanaras, A. G.; Sönnichsen, C.; Liu, H.; Alivisatos, A. P. *Nano Lett.* **2005**, *5*, 2164.
(9) Vlasov, Y. A.; Astratov, V. N.; Karimov, O. Z.; Kaplyanskii, A. A.; Bogomolov, V. N.; Prokofiev, A. V. *Phys. Rev. B* **1997**, *55*, 13357.
(10) (a) Attard, G. S.; Glyde, J. C.; Goltner, C. G. *Nature* **1995**, *378*, 366. (b) Pai, R. A.; Humayun, R.; Schulberg, M. T.; Sengupta, A.; Watkins, J. J. *Science* **2004**, *303*, 507. (c) Lee, K. B.; Lee, S. M.; Cheon, J. *Adv. Mater.* **2001**, *13*, 517.

 Published on Web 06/28/2010 © 2010 American Chemical Society

crystal fiber structures with pores of 50 nm diameter which are greater than 1 m long.[12,13]

One technique for filling nanostructured templates which has had considerable success is supercritical chemical fluid deposition (SCFD). This technique exploits the unique properties of supercritical fluids, including zero surface tension, gas-like mass transport rates and the ability to act as a solvent to enable the filling of high aspect ratio pores, particularly nanopores. One key success of this technique is deposition of Cu into high aspect ratio 100 nm wide trenches in silicon wafers for next generation interconnects.[14] This work has since been extended to a wide range of metals including Ni, Au, Ru, Co, Rh, and Ir.[14,15] Another impressive result is the filling of 3−10 nm diameter pores in mesoporous silica with metals such as Cu and the elemental semiconductors Si and Ge, to form continuous tubes or wires with no detectable central void.[16] SCFD has also been shown to be particularly effective at depositing a range of metals, polymers and elemental semiconductors into photonic crystal fibers enabling a new generation of photonic devices including chemical sensors[12] and optical modulators.[13]

The application of SCFD to the deposition of high quality direct bandgap semiconductors such as the III−V semiconductors would clearly lead to some important and technologically interesting nanostructures. However there has only been limited work on SCFD of compound semiconductors in general and even less on III−V semiconductors in particular. The most developed supercritical fluid based semiconductor deposition method is the ammonothermal growth of bulk GaN on seed crystals, in which epilayers of GaN are produced using either Ga or GaN as the gallium source.[17] The aggressive nature of supercritical ammonia means that this method is only suitable for depositing nitride semiconductors and the use of solid gallium sources means extending it to produce even nitride heterostructures would be challenging. GaP has previously been produced using a supercritical fluid to deliver precursors to a conventional CVD chamber, followed by the rapid expansion of the fluid onto the heated substrate.[18] However, the only published work on III−V deposition directly from a supercritical fluid involves the production of GaP[19] and GaAs[20] nanowires using a method analogous to vapor−liquid−solid growth called supercritical-fluid-liquid solid growth (SFLS). The SFLS method used is effectively a close analogue of MOCVD/CVD and the reagents used were $^{t}Bu_3Ga$, $P(SiMe_3)_3$ and $As(SiMe_3)_3$. The wires produced were characterized in terms of their conductance but not charge carrier mobility or luminescence. Most recently CdS, has been deposited using SCFD in a flow reactor,[21] the first case of II−VI semiconductor deposition in this way. The material deposited was a polycrystalline layer which demonstrated good quality band-edge luminescence with a line width narrower than that of pulsed laser deposited material which has been shown to lase.

In this paper we present the growth of III−V films and nanowires from SCFs. This was expected to be significantly more challenging than growth of CdS. The reagents available for III−V growth are typically very sensitive to oxygen and moisture. The luminescence and transport properties of the semiconductors themselves are also very sensitive to impurities, including oxygen. The exposure of the precursor to the carrier fluid is clearly more significant in SCFD than in low pressure (LP)CVD with a carrier gas, so a significant concern was that the purity of fluid needed for high quality deposition would be unachievable. Dimeric $[R_2In(\mu\text{-}ER'_2)_2InR_2]$ compounds (E = P, As; R, R′ = alkyl) were selected as precursors to InP and InAs because they are less oxygen sensitive and hence easier to handle than the pyrophoric indium alkyls and highly toxic PH_3 and AsH_3 gases typically used in dual source deposition. $[R_2Ga(\mu\text{-}As^{t}Bu_2)_2GaR_2]$ (R = Me, ^{i}Pr, ^{t}Bu) have been used to grow n- (Me) or p-type (^{i}Pr, ^{t}Bu) GaAs by LPCVD including epitaxial films.[22,23] Cowley and co-workers developed a series of such dimeric precursors containing Al, Ga or In with dialkyl-phosphido or -arsenido bridging ligands.[24−26] We considered $[^{n}Bu_2In(\mu\text{-}P^{t}Bu_2)_2In^{n}Bu_2]$[25] to be a promising precursor for SCFD because the alkyl chains impart good solubility in nonpolar solvents and often this is a good indicator of likely solubility in supercritical CO_2. Hence this compound and its arsenido

(11) Baker, G.; Hix, G.; Ouali, F. *Zeolite-Semiconductor Composites*; lecture presented at British Zeolite Association's 33rd Annual Meeting; Southampton, U.K., March 26, 2010.
(12) Amezcua-Correa, A.; Yang, J.; Finlayson, C. E.; Peacock, A. C.; Hayes, J. R.; Sazio, P. J. A.; Baumberg, J. J.; Howdle, S. M. *Adv. Funct. Mater.* **2007**, *17*, 2024.
(13) Won, D. J.; Ramirez, M. O.; Kang, H.; Gopalan, V.; Baril, N. F.; Calkins, J.; Badding, J. V.; Sazio, P. J. A. *Appl. Phys. Lett.* **2007**, *91*, 161112.
(14) Blackburn, J. M; Long, D. P.; Cabanas, A.; Watkins, J. J. *Science* **2001**, *293*, 141.
(15) (a) Long, D. P.; Blackburn, J. M.; Watkins, J. J. *Adv. Mater.* **2000**, *12*, 913. (b) O'Neil, A.; Watkins, J. J. *Chem. Mater.* **2006**, *18*, 5652. (c) O'Neil, A.; Watkins, J. J. *Green Chem.* **2004**, *6*, 363. (d) Momose, T.; Sugiyama, M.; Kondoh, E.; Shimogaki, Y. *Appl. Phys. Exp.* **2008**, *1*, 097002. (e) Kondoh, E.; Kato, H. *Microelectron. Eng.* **2002**, *64*, 495.
(16) Holmes, J. D.; Johnston, K.; Doty, R.; Korgel, B. *Science* **2000**, *287*, 1471. (b) Lin, C.; Lam, F.; Hu, X.; Tam, W.; Ng, K. *J. Phys. Chem. C* **2008**, *112*, 10068. (c) Holmes, J. D.; Lyons, D. M.; Ziegler, K. J. *Chem. Eur. J.* **2003**, *9*, 2144.
(17) Hashimoto, T.; Wu, F.; Speck, J. S.; Nakamura, S. *Nat. Mater.* **2007**, *6*, 568.
(18) Popov, V. K.; Bagratashvili, V. N.; Antonov, E. N.; Lemenovski, D. A. *Thin Solid Films* **1996**, *279*, 66.
(19) Davidson, F. M., III; Wiacek, R.; Korgel, B. A. *Chem. Mater.* **2005**, *17*, 230.
(20) Davidson, F. M., III; Schricker, A. D.; Wiacek, R.; Korgel, B. A. *Adv. Mater.* **2004**, *16*, 647.
(21) Yang, J.; Hyde, J. R.; Wilson, J. W.; Mallik, K.; Sazio, P. J. A.; O'Brien, P.; Malik, M. A.; Afzaal, M.; Nguyen, C. Q.; George, M. W.; Howdle, S. M.; Smith, D. C. *Adv. Mater.* **2009**, *21*, 4115.
(22) Cowley, A. H.; Jones, R. A. *Angew. Chem., Intl. Ed.* **1989**, *28*, 1208.
(23) Cowley, A. H.; Jones, R. A. *Polyhedron* **1994**, *13*, 1149.
(24) Arif, A. M.; Benac, B. L.; Cowley, A. H.; Geerts, R.; Jones, R. A.; Kidd, K. B.; Power, J. M.; Schwab, S. T. *J. Chem. Soc., Chem. Commun.* **1986**, 1543.
(25) Atwood, D. A.; Atwood, V. O.; Cowley, A. H.; Gobran, H. R.; Jones, R. A. *Organometallics* **1993**, *12*, 3517.
(26) (a) Arif, A. M.; Benac, B. L.; Cowley, A. H.; Jones, R. A.; Kidd, K. B.; Nunn, C. M. *New J. Chem.* **1988**, *12*, 553. (b) Miller, J. E.; Kidd, K. B.; Cowley, A. H.; Jones, R. A.; Ekerdt, J. G.; Gysling, H. J.; Wernberg, A. A.; Blanton, T. N. *Chem. Mater.* **1990**, *2*, 589. (c) Atwood, D. A.; Cowley, A. H.; Harris, P. R.; Jones, R. A.; Koschmieder, S. U.; Nunn, C. M. *J. Organomet. Chem.* **1993**, *449*, 61. (d) Cowley, A. H.; Corbelin, S.; Jones, R. A.; Lagow, R. L.; Nail, J. W. *J. Organomet. Chem.* **1994**, *464*, C1.

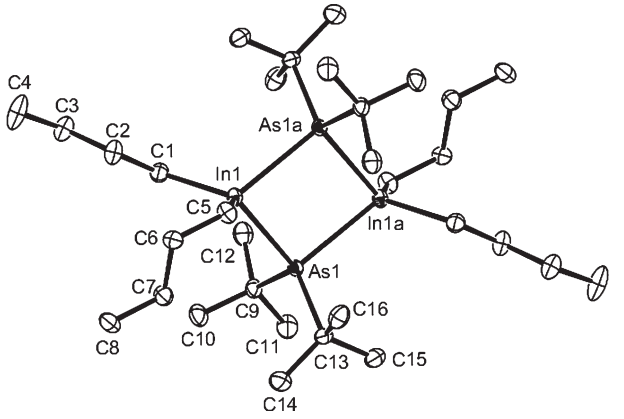

Figure 1. View of the structure of the centrosymmetric [^{n}Bu$_2$In(μ-As^{t}Bu$_2$)$_2$In^{n}Bu$_2$] with atom numbering scheme. Ellipsoids are shown at the 50% probability level. Symmetry operation: $a = 1-x, 1-y, 1-z$. The same numbering scheme applies to the isomorphous [^{n}Bu$_2$In(μ-P^{t}Bu$_2$)$_2$In^{n}Bu$_2$].

Table 1. Selected Bond Lengths (Å) and Angles (deg) for [^{n}Bu$_2$In(μ-E^{t}Bu$_2$)$_2$In^{n}Bu$_2$]^a

	E = P	E = As
In1−C1	2.2090(14)	2.200(3)
In1−C5	2.2032(14)	2.196(3)
In1−E1	2.6552(7)	2.7203(6)
In1−E1a	2.6541(7)	2.7197(6)
C1−In1−C5	114.40(5)	116.57(13)
C1−In1−E1a	112.16(4)	111.75(10)
C5−In1−E1a	111.18(4)	111.33(9)
C1−In1−E1	111.40(4)	111.18(9)
C5−In1−E1	119.17(4)	118.40(10)
E1−In1−E1a	84.997(18)	82.804(17)
In1−E1−In1a	95.003(18)	97.196(17)

^{a} Symmetry operation: $a = 1-x, 1-y, 1-z$.

analogue were synthesized and used in the deposition studies described herein.

Results and Discussion

The reagents [^{n}Bu$_2$In(μ-E^{t}Bu$_2$)$_2$In^{n}Bu$_2$] (E = P or As) were obtained in good yield by a modification of the method developed by Cowley and co-workers for the corresponding [^{n}Bu$_2$Ga(μ-E^{t}Bu$_2$)$_2$Ga^{n}Bu$_2$].[24] The resulting white powdered solids were stored and manipulated in an N_2 purged, dry (< 1 ppm H_2O) glovebox and were characterized by ^{1}H and ^{31}P{^{1}H} NMR spectroscopy, microanalysis and single crystal X-ray analysis. The structures are isomorphous (Figure 1 and Table 1) and confirm the expected centrosymmetric dimers, with the phosphide or arsenide ligands bridging symmetrically between the In centers, and d(In−P) slightly shorter than d(In−As).

Deposition of InP. For comparison with the SCFD studies, LPCVD from [^{n}Bu$_2$In(μ-P^{t}Bu$_2$)$_2$In^{n}Bu$_2$] was also attempted. The growth of InP from related precursors (different substituents) under LPCVD conditions has previously been claimed,[22,27,28] though characterization of the films was reported only in one case, [Me$_2$In(μ-P^{t}Bu$_2$)$_2$InMe$_2$], in which InP was found to be contaminated with In metal unless dissociated PH_3 was added simultaneously to the growth chamber.[27] Films were grown on silica tiles at temperatures between 723 and 873 K. SEM showed films with nanoparticles attached to the surface. EDX analysis suggested an indium rich composition (In:P ~1.1:1).

X-ray diffraction patterns showed cubic InP, but also indium metal at all temperatures, with a large amount of indium metal observed in films grown at 723 K but much less at 823 or 873 K. This is similar to the reported behavior of [Me$_2$In(μ-P^{t}Bu$_2$)$_2$InMe$_2$].[27] WDX showed In:P ratios close to 1:1 in films grown at 723 or 773 K, but indium-rich compositions at other temperatures and carbon contents of 10−27 at %. No photoluminescence could be observed from any of these films under the conditions used to study the SCFD-derived ones.

Solubility in nonpolar solvents such as hexane is normally considered a good indicator of likely solubility in supercritical CO_2. However, using a flow reactor with flowing CO_2, [^{n}Bu$_2$In(μ-P^{t}Bu$_2$)$_2$In^{n}Bu$_2$] was found to be poorly soluble and it was not possible to transport the precursor to the heated substrate for film growth. When the precursor was simply placed in a batch reactor and pressurized with CO_2 before heating the reactor with static fluid, very thin substrate-colored films were obtained. EDX showed these to contain In and P but no crystalline material was observed in the X-ray diffraction patterns. Powdered material left in the reactor where the precursor was introduced did contain cubic InP, but also In metal and other unidentified impurities. It is clear that the precursor is insufficiently soluble in supercritical CO_2 so most of it decomposes by pyrolysis as the solid and only a very small amount is transported to the substrate.

To achieve better solubility of the precursor in the SCF, the precursor was introduced to the reactor as a hexane solution before pressurization with CO_2. The quantities of hexane and CO_2 used were calculated to ensure a single phase supercritical fluid was maintained above a critical point of 512 K and 4.4 MPa pressure.[29] Under these conditions, thicker films of cubic InP containing little or no impurity by XRD could be obtained, but these were dull and powdery, indicating significant particulate deposition. On the basis that this material was likely to result from homogeneous decomposition of the precursor in the hot wall reactor, some dried glass wool was placed in the bottom of the reactor to adsorb particles from the solution. This inhibited deposition of particles on the substrate and shiny, reflective InP films were then obtained.

The best InP films, which were cubic and exhibited good band-edge luminescence (see later), were grown from 0.10 g of precursor with a furnace temperature of

(27) Andrews, D. A.; Davies, G. J.; Bradley, D. C.; Faktor, M. M.; Frigo, D. M.; White, E. A. D. *Semicond. Sci. Technol.* **1988**, *3*, 1053.
(28) Cowley, A. H.; Benac, B. L.; Ekerdt, J. G.; Jones, R. A.; Kidd, K. B.; Lee, J. Y.; Miller, J. E. *J. Am. Chem. Soc.* **1988**, *110*, 6248.
(29) Lemmon, E. W., Huber, M. L., McLinden, M. O. *NIST Standard Reference Database 23: Reference Fluid Thermodynamic and Transport Properties-REFPROP, Version 8.0*; National Institute of Standards and Technology: Gaithersburg, MD, 2007.

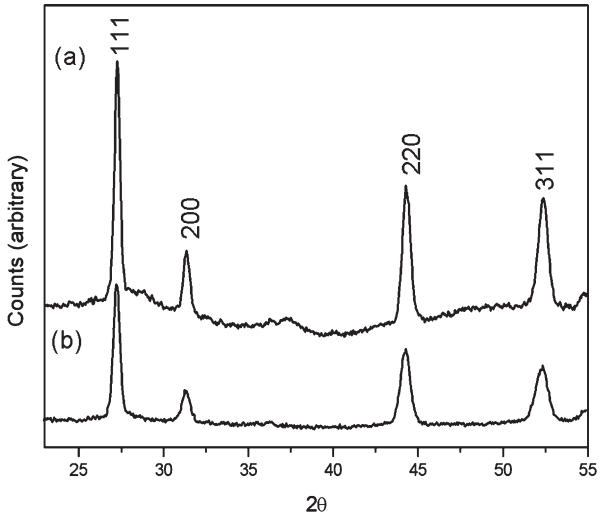

Figure 2. X-ray diffraction patterns of a cubic InP film grown at 773 K for 18 h from hexane/CO_2 (a) with InP wires attached and (b) after the InP wires were removed. Miller indices denote reflection positions associated with cubic InP.

773 K (691 K at substrate) over a period of 18 h. These were shiny and optically thin with a greenish tinge to the substrate color. Shorter periods of growth, of 2 or 4 h, resulted in shiny green films of very similar thickness, morphology and crystallinity but with much poorer photoluminescence than the films heated for the longer period. Since the addition of excess ^{n}BuSH resulted in improved photoluminescence in the growth of CdS,[21] film growth with a small excess (1.4 mol equiv) of ^{t}Bu$_2$PH was also trialed. The effect was to reduce the film thickness, increase the amount of amorphous material observed by PXD and increase broad band luminescence relative to band-edge. Increasing the deposition temperature to 823 K (758 K at substrate) produced films of similar thickness to those grown at 773 K but broadened X-ray diffraction peaks were observed, corresponding to *ca* 35 nm crystallites and the nanowires were narrower. This suggests that nucleation occurs readily at the higher temperature. Growth at 723 K (639 K at substrate) yielded cubic InP films, but with a different morphology – ~1 μm particles were observed with few nanowires. At 723 and 823 K, the band-edge luminescence was significantly lower in intensity relative to broad band emission than at 773 K, therefore our main characterization efforts focused on films grown under these conditions.

The X-ray diffraction patterns of the films grown at 773 K for 18 h, Figure 2, showed cubic InP with a lattice parameter of 5.860(23) Å and fwhm of 0.35° for the 111 reflection, corresponding to a lattice coherence length (often referred to as crystallite size) of ca. 90 nm, and comparable with the thicknesses of the nanowires observed on the surface that are evident by SEM (Figure 3). These wires grew to a film thickness of around 2 μm. The

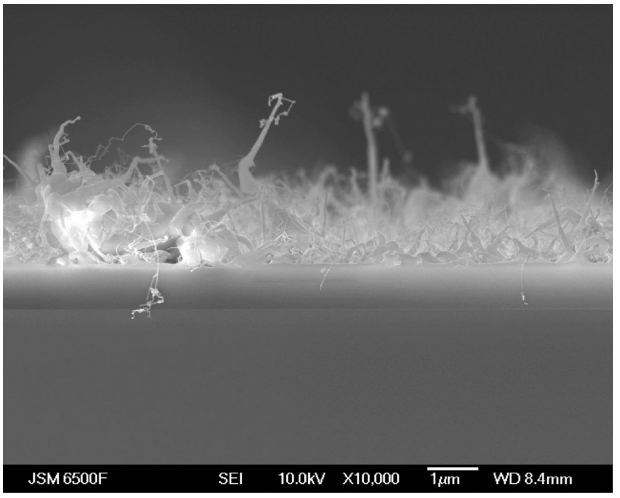

Figure 3. SEM image of a cubic InP film and nanowires grown at 773 K for 18 h from hexane/CO_2, attached to the surface of a cleaved silicon wafer substrate.

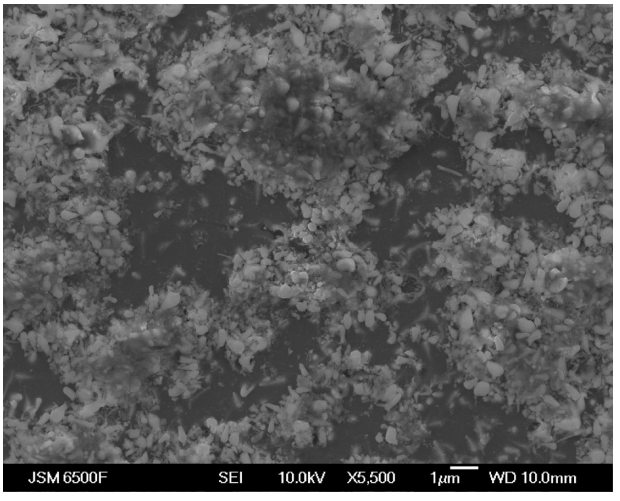

Figure 4. SEM image of a cubic InP film grown at 773 K for 18 h from hexane/CO_2, after the nanowires had been removed by gentle rubbing with a cotton bud.

lattice parameter is close to reported values for InP, which range from 5.87 to 5.88 Å.[30] Most of the wires could be removed by wiping gently with a cotton bud, leaving a 350 nm thin film (Figure 4). X-ray diffraction after removing the wires (Figure 2) still showed cubic InP (5.868(41) Å) but the amorphous material, observed via the sloping baseline in the pattern taken with the wires in place, was no longer present. The line-width remained the same. WDX showed highly consistent In:P ratios of 1.16:1 over a series of sample analysis positions with wires and after wire removal, with average carbon contents of 17 at %, and EDX spot scans at various positions gave similar results. Hence, the films are slightly In-rich and the compositions of the wiry material and the underlying film are not markedly different.

Examination of a sample by TEM showed nanowires in two distinct size ranges (Figure 5). Nanowires of ca. 60 nm diameter and lengths of up to 1.2 μm were observed, with lattice fringes showing growth along [111]. Selected area electron diffraction identified a single-crystal structure.

(30) Values taken from the PDF database citing the following papers: (a) Antyukhov, A. M. *Inorg. Mater.* **1986**, *22*, 426. (b) Geist, V.; Ascheron, C. *Cryst. Res. Technol.* **1984**, *19*, 1231. Giesecke, G.; Pfister, H. *Acta Crystallogr.* **1958**, *11*, 369. (c) Koester, W.; Ulrich, W. *Z. Metallkd.* **1958**, *49*, 365.

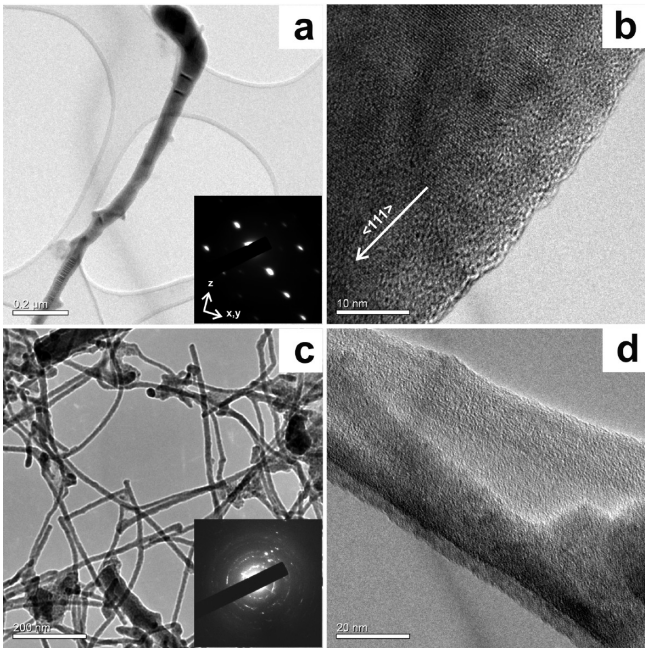

Figure 5. TEM images of InP wires of different sizes grown at 773 K for 18 h from hexane/CO_2: (a, b) individual single-crystal nanowire of ca. 60 nm diameter and growing along [111] (scale bars 200 and 10 nm); (c, d) polycrystalline nanowires of ca. 15 nm diameter (scale bars 200 and 20 nm).

The wires have a rough amorphous surface and it is likely that at least some of the amorphous material observed in the XRD patterns is coated onto the surface of the wires. Further nanowires with diameters of ca. 15 nm and lengths of up to at least 1 μm were polycrystalline. TEM showed these were wires with noncontinuous lattice planes and amorphous regions. Selected area electron diffraction showed polycrystalline patterns (rings), though these were textured with bright spots, suggesting a small number of crystallites.

Nanowires have been shown to grow from liquid nanoscale seeds formed from the components of the semiconductor mixed with a metal to produce a liquid droplet. The semiconductor precursors feed the components of the semiconductor into the droplet causing the semiconductor to precipitate onto the end of the wire. This mechanism is referred to as vapor− and solution−liquid−solid (VLS and SLS) growth depending on the growth environment.[3,4] The growth of single crystal wires might suggest a similar mechanism is at work here. The evidence of elemental In in the CVD films supports that possibility that excess indium could be present to form liquid nanoscale seeds. However, no elemental indium was found in the SCFD films and TEM images of the nanowires do not show residual metal particles at the end of the nanowires. It may be that such In-rich droplets do form but are incorporated or evaporate at the end of the growth, or that another as yet unknown mechanism is responsible.

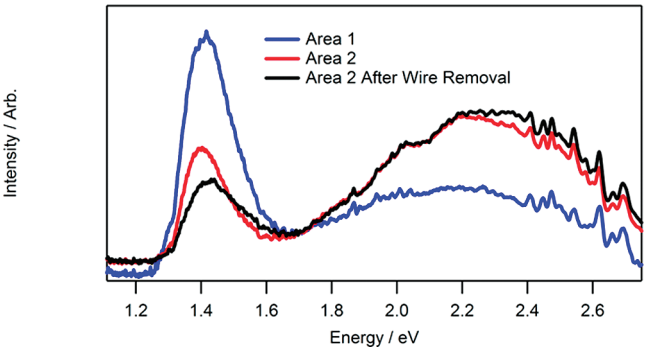

Figure 6. Room-temperature PL spectra of cubic InP films grown at 773 K for 18 h from hexane/CO_2 showing the variation between two areas and the minimal effect of removing the wires.

Representative room-temperature photoluminescence spectra are presented in Figure 6. The spectra have two main features, a peak at 1.42 eV with a fwhm of 0.16 eV, consistent with band edge luminescence,[31] and a broad supra-bandgap emission from 1.7 to 2.7 eV. Luminescence in this region has previously been attributed to the presence of oxygen compounds in spark-processed porous InP.[32] In_2O_3 prepared by the oxidation of In films is also known to exhibit luminescence at this energy.[33] The sharp lines superimposed on this broad emission are attributed to the excitation source. The wires removed by abrasion with a cotton bud could not be recovered. More vigorous scraping led to the underlying film being removed. Attempts to recover sufficient wires after their removal by the application of ultrasound in a solvent were also unsuccessful. Thus it was not possible to measure PL from the wires separate from the underlying films. However since SEM shows these films to be dense and thicker than the absorption length of InP at the excitation wavelength, ~100 nm, we believe that the luminescence in the unwiped samples is predominantly from the InP wires.

The high carbon contents of InP films produced in hexane/CO_2 mixtures could be due to solvent decomposition or to incomplete loss of substituent groups from the precursor compounds that then leads to pyrolysis and deposition of carbon. Deposition from a solvent that was considered less likely to decompose under the deposition conditions, supercritical CHF_3, was tried to determine whether the carbon contents could be reduced. Films were grown at 773 K (693 K at substrate) and 4 MPa using the same reactor design as used in the hexane/CO_2 depositions. Black films, with green or purple fringes in thinner areas, were obtained, but only on the part of the substrate closest to the precursor, suggesting limited solubility.

XRD patterns of these samples showed cubic InP (a = 5.895 Å) with a similar line width to that discussed above. SEM (Figure 7) showed a solid film and long nanowires attached to it. WDX showed slightly In rich films (In:P 1.07:1, consistent with EDX), and although carbon

(31) (a) Roder, O.; Heim, U.; Pilkuhn, M. H. *J. Phys. Chem. Solids* **1970**, *31*, 2625. (b) Wang, F.; Yu, H.; Li, J.; Hang, O. Q.; Zemlyanov, D.; Gibbons, P. C.; Wang, L.-W.; Janes, D. B.; Buhro, W. E. *J. Am. Chem. Soc.* **2007**, *129*, 14327.

(32) Rojas-Lopez, M.; Nieto-Navarro, J.; Rosendo, E.; Navarro-Contreras, H.; Vidal, M. A. *Thin Solid Films* **2000**, *379*, 1.

(33) Lee, M.-S.; Choi, W. C.; Kim, E. K.; Kim, C. K.; Min, S. K. *Thin Solid Films* **1996**, *279*, 1.

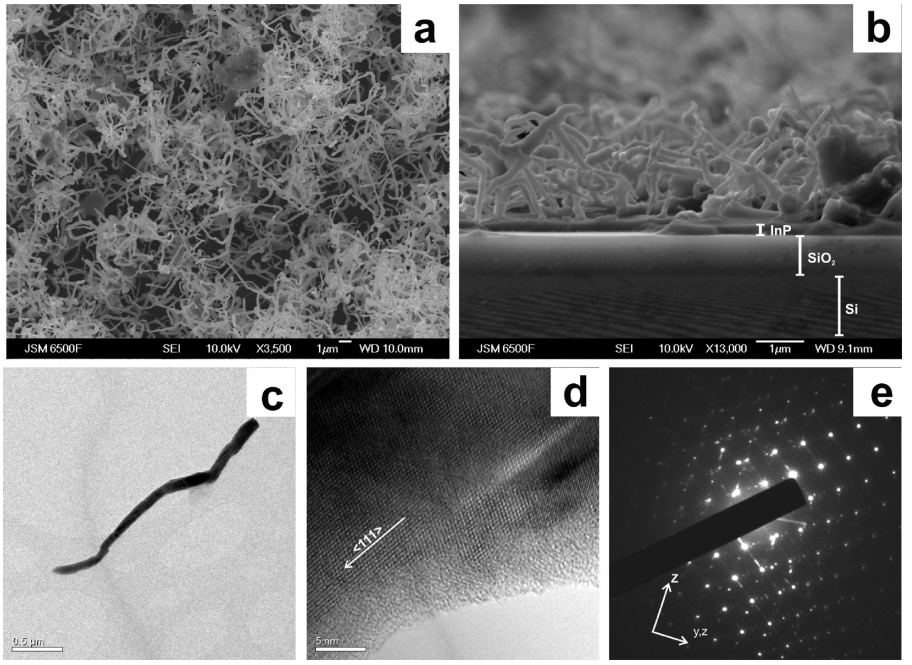

Figure 7. SEM images of cubic InP film grown from CHF_3 and nanowires attached on the surface: (a) top view (1 μm scale bar), (b) side view after cleaving the Si wafer (1 μm scale bar). TEM images: (c) individual InP nanowire (500 nm scale bar), (d) HRTEM representative image of InP wire (5 nm scale bar), (e) SAED patterns indicating InP nanowires exhibiting preferential orientation along [111].

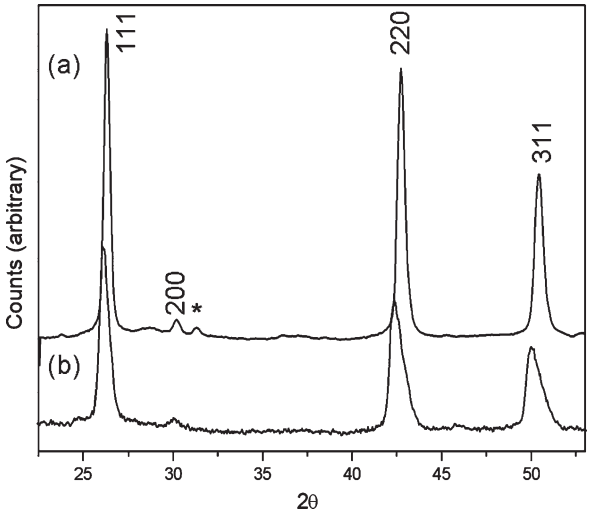

Figure 8. X-ray diffraction patterns of cubic InAs films grown by SCFD at 823 K for 18 h (top) and by LPCVD at 723 K (bottom). Miller indices denote the positions of reflections in the InAs lattice and the asterix the strongest reflection of In.

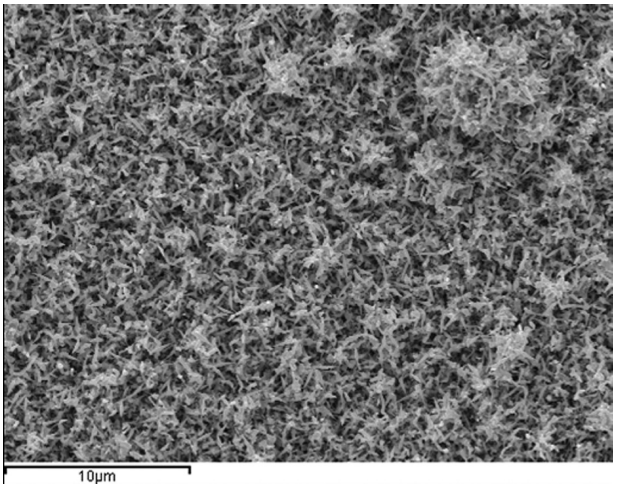

Figure 9. SEM image of a cubic InAs film grown by LPCVD at 723 K.

contents were variable, the lowest still contained 9 at % C averaged across several regions of the film, suggesting that the precursor is responsible at least for some of the carbon contamination. TEM showed these wires to have a single crystalline core (lattice fringes and spot pattern in Figure 8) with a polycrystalline/amorphous shell. Photoluminescence spectra were similar to those shown in Figure 6. It is possible that the lower solubility of the precursor in this fluid results in slower growth and hence exclusively single-crystal wires, but otherwise the films were very similar to those grown from CO_2/hexane.

Deposition of InAs. LPCVD from [^{n}Bu$_2$In(μ-As^{t}Bu$_2$)$_2$-In^{n}Bu$_2$] at 723 or 773 K resulted in cubic InAs films, Figure 8, with a = 6.127(5) or 6.097(11) Å respectively. Typical values for bulk InAs are 6.058−6.062 Å.[34] Unlike the analogous InP growth, no indium metal was observed. However, the films were powdery and poorly adhered. SEM showed a similar surface morphology to that found with InP, a mat of wires was growing on the surface of the substrate (Figure 9).

SCFD yielded matt gray films at 773 or 823 K. SEM showed these to consist of around 120−140 nm diameter

(34) Values taken from the PDF database citing the following papers: (a) Massidda, S.; Continenza, A.; Freeman, A. J.; de Pascale, T. M.; Meloni, F.; Serra, M. *Phys. Rev. B: Condens. Matter* **1990**, *41*, 12079. (b) Katayama, I.; Nakai, T.; Inomoto, T.; Kozuka, Z. *Trans. Jpn. Inst. Met.* **1989**, *30*, 354. (c) Antyukhov, A. M. *Inorg. Mater.* **1986**, *22*, 426. (d) Drobayzko, V. P.; Kuznetsova, S. T. *Russ. J. Inorg. Chem.* **1983**, *28*, 1660. (e) Morozov, V. N.; Chernov, V. G. *Inorg. Mater.* **1979**, *15*, 1036. (f) Drobayzko, V. P.; Kuznetsova, S. T. *Russ. J. Inorg. Chem.* **1975**, *20*, 1693.

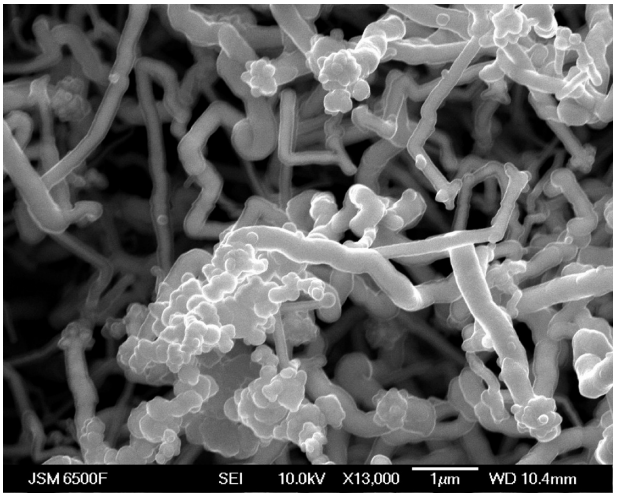

Figure 10. SEM image of cubic InAs loosely attached to a silicon substrate. This sample was grown by SCFD at 823 K.

nanowires forming a poorly adhered mat 1.5−2.0 μm thick, but unlike with InP only a very thin, shiny, underlying solid film of ca. 30 nm was observed. PXD showed the 773 K film to contain cubic InAs with some In_2O_3, but that the films grown at 823 K consisted only of cubic InAs with $a = 6.096(11)$ Å and just a trace of In metal (Figure 8). The crystallite sizes calculated from the PXD linewidths were 31 nm (773 K) and 54 nm (823 K). The wires (Figure 10) were again poorly adhered, and tapping the substrate on a solid surface was sufficient to detach most of the material. EDX showed a 1:1 ratio of In:As at both temperatures.

Conclusions

Supercritical chemical fluid deposition from [^{n}Bu$_2$In(P^{t}Bu$_2$)$_2$In^{n}Bu$_2$] and [^{n}Bu$_2$In(As^{t}Bu$_2$)$_2$In^{n}Bu$_2$] results in InP and InAs. These encouraging results show that III−V semiconductors can be deposited from single phase supercritical fluids and that the method is generally applicable following previous depositions of CdS, even where the use of highly moisture or oxygen sensitive reagents is required. The band edge luminescence exhibited by InP shows the presence of significant quantities of pure, high quality InP. Considering the usefulness of the method for filling or conformal coating of small, high-aspect-ratio features, the deposition of direct bandgap semiconductors is significant. The reagents used in this study appear to have contributed significantly to the contamination of the products with carbon, as does the hexane co-solvent used for much of the work. Changes to the precursor system, combined with the use of fluorinated fluids and a cool walled flow-reactor layout (to minimize homogeneous growth), are likely to allow the growth of high-purity III−V materials by SCFD in the future.

Experimental Section

All reactions were conducted using Schlenk, vacuum line and glovebox techniques and under a dry nitrogen atmosphere. [^{n}Bu$_2$In(E^{t}Bu$_2$)$_2$In^{n}Bu$_2$] (E = P, As) were prepared by a method analogous to that published for the preparation of [^{n}Bu$_2$Ga(E^{t}Bu$_2$)$_2$Ga^{n}Bu$_2$] (E = P, As).[35] Hexane, toluene, diethyl ether and THF were dried by distillation over sodium/benzophenone. $InCl_3$, ^{n}BuLi, ^{t}BuLi, $AsCl_3$, and HP^{t}Bu$_2$ were obtained from Aldrich and used as received. LiP^{t}Bu$_2$, HAs^{t}Bu$_2$, and LiAs^{t}Bu$_2$ were prepared according to the method of Holga et al.[36]

[^{n}Bu$_2$In(P^{t}Bu$_2$)$_2$In^{n}Bu$_2$]. A solution of LiP^{t}Bu$_2$ (0.600 g, 3.94 mmol) in THF (40 mL) was added dropwise to a solution of $InCl_3$ (0.872 g, 3.94 mmol) in THF (15 mL) at 196 K. The mixture was allowed to warm to room temperature and reacted for 2 h, and then cooled back to 196 K and a solution of 1.6 M ^{n}BuLi (4.93 mL, 7.89 mmol) was added dropwise. The mixture was stirred overnight at room temperature. THF was removed under a vacuum and the residue extracted into hexane (3 × 10 mL) and then filtered. The volume of the filtrate was reduced to approximately 5 mL and cooled (253 K) overnight. The colorless crystals were collected, washed with hexane (1 mL), and dried under a vacuum. Yield: 2.0 g (40.8%). ^{31}P{^{1}H} NMR (C_6D_6): δ 44.8. ^{1}H NMR (C_6D_6): δ 1.07 (t, 12H), 1.60 (m, 8H), 1.91 (m, 8H) (all ^{n}Bu), 1.36 (t, 36H, ^{t}Bu$_2$P). Anal. Calcd for $C_{32}H_{72}In_2P_2$: C, 51.4; H, 9.7. Found: C, 51.7; H, 9.7.

[^{n}Bu$_2$In(As^{t}Bu$_2$)$_2$In^{n}Bu$_2$]. Prepared in the same manner using LiAs^{t}Bu$_2$, $InCl_3$, and ^{n}BuLi. Yield: 36.5%. ^{1}H NMR (C_6D_6): δ 1.07 (t, 12H), 1.21 (m, 8H), 1.60 (m, 8H), 1.93 (m. 8H) (all ^{n}Bu), 1.43 (s, 36H, ^{t}Bu$_2$). Anal. Calcd for $C_{32}H_{72}In_2As_2$: C, 45.0; H, 8.7. Found: C, 45.8; H, 8.7.

LPCVD from [^{n}Bu$_2$In(E^{t}Bu$_2$)$_2$In^{n}Bu$_2$] (E = P, As). 0.100 g of reagent and silica substrates were loaded into a quartz tube in a glovebox. The tube was then set in a furnace and evacuated, then heated to achieve deposition at 773 K under 0.05 mmHg (66 Pa). The sublimation temperature of the reagents was approximately 433 K.

SCFD from [^{n}Bu$_2$In(E^{t}Bu$_2$)$_2$In^{n}Bu$_2$] (E = P, As). Under an inert atmosphere, 0.100 g of reagent dissolved in 14 mL of dry hexane was added to a glass tube sealed at one end containing a Si/SiO_2 substrate (IDB Technologies, 3″, <N100>, 950 ± 10 nm SiO_2) raised on glass wool. The glass tube was inserted into a 316 L stainless steel pressure vessel which was then sealed. The reactor was set in a furnace and connected to a Peltier chilled HPLC pump (Jasco, PU-2080-CO_2) and back pressure regulator (Jasco, BP-2080). The system was pressurized to 2 MPa with CO_2 (BOC Special Products, N5.5 grade) at room temperature. The system was heated to reaction temperature and allowed to pressurize to 12 MPa, controlled by the back pressure regulator. After the desired reaction time, the temperature was reduced to 473 K, CO_2 was flowed at 1.0 mL min^{-1} and the pressure maintained at 12 MPa for 4 h to extract the solvent. After extraction, the system was depressurized and allowed to cool to room temperature before the reactor was transferred to a glovebox for disassembly.

An identical system was used for InP deposition in CHF_3 (trifluoromethane, 98%, Sigma Aldrich). The 0.100 g of reagent and Si/SiO_2 substrate was placed in the glass tube, which was loaded in to the stainless steel pressure vessel. The sealed reactor was connected to the high-pressure system and pressurized with CHF_3 to 4 MPa. The system was heated to the reaction temperature. After the desired reaction time, the system was cooled to 350 K and depressurized via the back pressure regulator. Once cool, the reactor was transferred to the glovebox, where the substrates were removed.

(35) Arif, A. M.; Benac, B. L.; Cowley, A. H.; Geerts, R.; Jones, R. A.; Kidd, K. B.; Power, J. M.; Schwab, S. T. *Chem. Commun.* **1986**, 1543.
(36) Holga, K. T.; George, C. *Organomet.* **1990**, *9*, 275.

Table 2. Crystallographic Parameters[a]

	[^{n}Bu$_2$In-(μ-P^{t}Bu$_2$)$_2$In^{n}Bu$_2$]	[^{n}Bu$_2$In-(μ-As^{t}Bu$_2$)$_2$In^{n}Bu$_2$]
formula	$C_{32}H_{72}In_2P_2$	$C_{32}H_{72}As_2In_2$
M	748.48	836.38
cryst syst	triclinic	triclinic
space group	$P\bar{1}$ (No. 2)	$P\bar{1}$ (No. 2)
a (Å)	9.152(2)	9.2590(15)
b (Å)	10.477(3)	10.5659(15)
c (Å)	10.525(3)	10.5790(15)
α (deg)	76.087(10)	76.177(10)
β (deg)	85.885(10)	73.420(10)
γ (deg)	73.315(10)	85.848(10)
U [Å^3]	938.3(4)	963.2(3)
Z	1	1
μ(Mo−K$_\alpha$) (mm^{-1})	1.331	2.919
total no. of reflections	17532	18900
R_{int}	0.024	0.045
no. of unique reflns	4307	4407
no. of params	171	171
R_1 [$I_o > 2\sigma(I_o)$]	0.016	0.035
R_1 (all data)	0.017	0.049
wR_2 [$I_o > 2\sigma(I_o)$]	0.047	0.059
wR_2 (all data)	0.048	0.065

[a] Common items: temperature = 120 K; wavelength (Mo−Kα) = 0.71073 Å; θ(max) = 27.5°; $R_1 = \Sigma||F_o| - |F_c||/\Sigma|F_o|$; $wR_2 = [\Sigma w(F_o^2 - F_c^2)^2/\Sigma wF_o^4]^{1/2}$.

Analytical. ^{1}H NMR spectra were recorded from solutions in C_6D_6 on a Bruker AV300, $^{31}P\{^1H\}$ NMR spectra on a Bruker DPX400 and referenced to 85% H_3PO_4. Microanalytical results were from the University of Strathclyde or Medac Ltd. XRD analysis was performed on a Bruker AXS D8 Discover with GADDS detector. SEM was performed on uncoated samples at an accelerating voltage of 10 kV using a JEOL JSM 6500F and EDX data were obtained with an Oxford INCA300 detector. TEM were collected with a Jeol JEM-3010 microscope operating at 300 kV using samples dispersed into methanol and deposited onto carbon grids. WDX data were outsourced to the Institute of Archaeology, University College London, and collected over multiple spots on each sample on a Jeol 8100 microprobe. Photoluminescence measurements were made with a 364 nm excitation from an Ar-ion laser (Spectra Physics, 2065−7S). A power density of 125 Wcm^{-2} was used. The emission was focused into an optical fiber and analyzed using a UV−visible spectrometer (Ocean Optics, HR4000).

X-ray Crystallography. Details of the crystallographic data collection and refinement parameters are given in Table 2. Crystals suitable for single-crystal X-ray analysis were obtained as described above for the bulk preparation, but were collected before the final washing and drying step. Data collections used a Bruker-Nonius Kappa CCD diffractometer fitted with monochromated Mo−K$_\alpha$ radiation (λ = 0.71073 Å), with the crystals held at 120 K in a nitrogen gas stream. Structure solution and refinement were straightforward,[26−28,37] with H atoms introduced into the models in idealized positions. Selected bond lengths and angles are given in Table 1.

CCDC-771205 and 771206 contain the supplementary crystallographic data for this paper. These data can be obtained free of charge from The Cambridge Crystallographic Data Centre via www.ccdc.cam.ac.uk/data_request/cif.

Acknowledgment. This work was funded by RCUK through Basic Technology programme EP/C006763/1. Thanks also to Prof. Ivan Parkin and Dr. Geoff Hyett for organizing the WDX measurements, Dr Mark Light for XRD training and maintenance, Dr Michael Webster for helping with the single crystal X-ray studies, and Profs. Michael George, Steven Howdle and Paul O'Brien for helpful discussions of SCFD.

(37) (a) Sheldrick, G. M. *SHELXS-97, Program for Crystal Structure Solution*; University of Göttingen: Göttingen, Germany, 1997. (b) Sheldrick, G. M. *SHELXL-97, Program for Crystal Structure Refinement*; University of Göttingen: Göttingen, Germany, 1997.; (c) Flack, H. D. *Acta Crystallogr., Sect. A* **1983**, *39*, 876–879.